

NACA RM L53J08a

7491



NACA

RESEARCH MEMORANDUM

CONTROL HINGE-MOMENT AND EFFECTIVENESS CHARACTERISTICS OF
SEVERAL INTERCHANGEABLE TIP CONTROLS ON A 60° DELTA
WING AT MACH NUMBERS OF 1.41, 1.62, AND 1.96

By Odell A. Morris

Langley Aeronautical Laboratory
Langley Field, Va.

NATIONAL ADVISORY COMMITTEE
FOR AERONAUTICS

WASHINGTON
November 25, 1953



NATIONAL ADVISORY COMMITTEE FOR AERONAUTICS

RESEARCH MEMORANDUM

CONTROL HINGE-MOMENT AND EFFECTIVENESS CHARACTERISTICS OF
SEVERAL INTERCHANGEABLE TIP CONTROLS ON A 60° DELTA
WING AT MACH NUMBERS OF 1.41, 1.62, AND 1.96

By Odell A. Morris

SUMMARY

Several tip controls have been investigated on a 60° delta wing to supplement information previously obtained with tip controls on the same wing plan form. Effects of changes in control leading-edge sweep and trailing-edge sweep on control hinge-moment and effectiveness characteristics were determined for both fence-off and fence-on conditions. Effects of skewing the 60° half-delta tip-control-wing combination were also determined. The aerodynamic characteristics of the complete wing-body combination, as well as the control hinge moments and bending moments, were obtained for an angle-of-attack range of $\pm 12^\circ$ and for control deflections up to 20° at Mach numbers of 1.41, 1.62, and 1.96, and Reynolds numbers of 2.4×10^6 , 2.25×10^6 , and 2.0×10^6 , respectively.

The results indicate that the nonlinear hinge-moment variations with deflection which appear to be associated with the angular gap between the wing and control forward of the hinge line were not improved by changes in control leading-edge sweepback from 60° to 75° , by changes in control trailing-edge sweep from -37.5° to 15° , or by $\pm 10^\circ$ skew of the control parting line and hinge line.

The balance characteristics at 0° control deflection and 0° angle of attack for the half-delta tip controls having the same hinge-line locations were essentially unchanged by variation of control leading-edge sweep angles from 45° to 75° .

The control effectiveness per unit area was little affected by increasing the control trailing-edge sweep to 15° , but was considerably decreased at angles of attack above zero by increasing the leading-edge sweep from 60° to 75° .

The only appreciable effects of wing skew were large negative increases in hinge moment at high angles of attack and positive control deflections when the wing panel was skewed back 10° .

INTRODUCTION

The half-delta tip control has been shown in wind-tunnel and free-flight tests to be a good lateral-control device at transonic and supersonic speed (refs. 1 to 3), and with the proper hinge-line location to have relatively low hinge moments over a limited Mach number range. For closely balanced tip controls, however, nonlinear variations of hinge moment occur with both angle of attack and deflection. The investigation of reference 4 has shown that the effects of control plan form on tip control balance characteristics were secondary to the ratio of control balance area to total area. The changes in control plan form in the tests of reference 4, however, did not alter the 60° delta wing plan form except in one case. It is, therefore, of interest to determine the effect of changes in control leading-edge and trailing-edge sweep angles on the nonlinear hinge-moment variations and the control balance characteristics as well as on the control effectiveness characteristics. In order to furnish such information, 45° half-delta, 60° triangular, and 75° half-delta tip controls mounted on a 60° delta wing have been tested with and without fences at the control-wing juncture in the Langley 9- by 12-inch supersonic blowdown tunnel at Mach numbers of 1.41, 1.62, and 1.96, and Reynolds numbers of 2.4×10^6 , 2.25×10^6 , and 2.0×10^6 , respectively.

The aerodynamic characteristics of the complete semispan model, as well as the control hinge moments and bending moments, were obtained through an angle-of-attack range of $\pm 12^\circ$ for control deflections up to 20° . Analysis of the data obtained for the 45° half-delta control was not made because large control torsional vibration occurred for some conditions. Data for the 60° half-delta control configuration of reference 1 are presented for purposes of comparison.

Also tests were made on a 60° half-delta control configuration with the complete wing skewed $\pm 10^\circ$ with respect to the body axis to obtain some preliminary knowledge of the effects of wing skew on control characteristics.

SYMBOLS

C_L	lift coefficient, $\frac{\text{Lift}}{qS}$
$C_{l_{\text{gross}}}$	gross rolling-moment coefficient about wind axes, $\frac{\text{Semispan wing rolling moment}}{2qSb}$

C_{BM_F}	control bending-moment coefficient about root chord of control surface, $\frac{\text{Bending moment}}{qS_F b_F}$
C_h	control hinge-moment coefficient about hinge line, $\frac{\text{Hinge moment}}{qS_F \bar{c}_F}$
$C_l, \Delta C_L$	increment in gross rolling-moment coefficient, and lift coefficient due to deflection of control surface
q	free-stream dynamic pressure
S	area of basic semispan wing with 60° half-delta control (including area blanketed by fuselage)
S_F	control-surface area
c	local wing chord
\bar{c}_F	mean aerodynamic chord of control
X_h	distance from hinge line to control leading edge measured along \bar{c}_F
b	wing span (twice distance from rolling-moment reference axis to wing tip with 60° half-delta control)
b_F	control surface span (distance from parting line to tip)
α	angle of attack measured with respect to free-stream direction
δ	control-surface deflection measured with respect to wing-chord plane
R	Reynolds number based on mean aerodynamic chord of wing
M	Mach number

Subscripts:

α	slope of curve of coefficient plotted against α ; for example, $C_{h_\alpha} = \frac{dC_h}{d\alpha}$
δ	slope of curve of coefficient plotted against δ ; for example, $C_{h_\delta} = \frac{dC_h}{d\delta}$

DESCRIPTION OF MODEL

The principal dimensions of the semispan delta wing model and the tip controls tested are shown in figure 1. A photograph of the model with the 60° half-delta control is shown in figure 2. The model had a leading-edge sweep of 60° and a corresponding aspect ratio of 2.3.

The main wing panel was made of solid steel and had modified hexagonal airfoil sections of constant thickness. The thickness ratio varied from 2.4 percent at the wing root to 9.2 percent at the wing control parting line. The wedge angles of the leading and trailing edges, measured parallel to the air stream, were 6.78° and 13.80° , respectively. The leading-edge wedge was modified by a small nose radius.

The 45° half delta, the two 60° triangular, and the 75° half-delta tip controls shown in figure 1(b) were tested during the present investigation. The 60° half-delta tip control shown in figure 1(a) was tested during the present investigation and also during the investigation reported in reference 1. The controls, which rotated about an axis in the wing perpendicular to the root chord, made up the outer portion of the wing and were separated from the inner wing panel by a streamwise parting line. The control surfaces had 3.0-percent-thick double-wedge airfoil sections and the leading edges were modified by a small nose radius. They were constructed of either solid steel or beryllium-copper. For part of the investigation a fence was mounted on the wing panel at the wing control parting line. The fence, dimensions of which are given in figure 1, was of sufficient size to seal the angular gap between the control surface and the wing panel at the highest deflection angles.

Details of the half fuselage (a body of revolution with a 0.25-inch shim), which was used in all of the tests, are also shown in figure 1.

TUNNEL

The tests were conducted in the Langley 9- by 12-inch supersonic blowdown tunnel, which is a nonreturn tunnel utilizing the compressed air from the Langley 19-foot pressure tunnel. The inlet air enters at an absolute pressure of about $2\frac{1}{3}$ atmospheres and contains about 0.3 percent of water by weight. The compressed air is conditioned to insure condensation-free flow in the test section by being passed through a silica gel dryer and then through banks of finned electrical heaters. Criteria for condensation-free flow were obtained from reference 5. Turbulence damping screens are located in the settling chamber. Interchangeable nozzle blocks provide three test-section Mach numbers.

Properties of the conditioned air and deviations from the average flow conditions in the test section with the tunnel clear, as determined from extensive calibration tests and reported in reference 6, are presented in the following table:

Variable	Nominal Mach number		
	1.41	1.62	1.96
Maximum deviation in Mach number	± 0.02	± 0.01	± 0.02
Maximum deviation in ratio of static to stagnation pressure, percent	± 2.0	± 1.3	± 2.2
Maximum deviation in stream angle, deg . .	± 0.25	± 0.20	± 0.20
Maximum dewpoint temperature, $^{\circ}\text{F}$	20	-5	-20
Minimum stagnation temperature, $^{\circ}\text{F}$	120	125	165

TEST TECHNIQUE

Semispan models are cantilevered from a five-component strain-gage balance mounted flush with the tunnel floor. The model rotates with the balance as the angle of attack is changed and the aerodynamic forces and moments on the wing-fuselage combination are measured with respect to the body axis and then rotated to the wind axis to determine the coefficients presented. For the skewed wing tests, the 60° delta wing was skewed $\pm 10^{\circ}$ from its original attitude with respect to the half body. The aerodynamic forces and moments were measured with respect to the same body axis, but in computing the data, the reference axes were rotated 10° to simulate the skewed positions. Angle-of-attack loading and body effects would not correctly simulate those of a wing in a yawed attitude, but for an outboard control at supersonic speeds, loading due to control δ should be approximately the same as if the complete model were yawed. In order to minimize the tunnel-wall boundary-layer effects on the flow over the cylindrical fuselage, models are shimmed out from the tunnel floor 0.25 inch (ref. 7). Because of balance deflection under load, a clearance gap of 0.010 to 0.020 inch is maintained between the fuselage shim and the tunnel floor.

The hinge moments and bending moments on the tip controls were measured by means of an optical system which was developed for use with wings too thin to permit conventional strain-gage installation.

The optical system consists primarily of two high intensity light sources mounted upon a large circular plexiglass screen with a radius of 80 inches, and two mirrors adjacent to each other (0.070 inch in diameter) installed flush in the model control surfaces and wing panel.

Reflection of the two light images upon the screen show the relative displacement of the tip light image with respect to the wing light image from which the hinge moments and bending moments may be determined. For a complete description of the optical system, see reference 1.

ACCURACY OF DATA

An estimate of the probable errors in the present data caused by the fluctuations in the readings of the measuring equipment, instrument reading errors, and calibration errors are presented in the following table:

Variable	Control plan form		
	60° half delta	60° triangular	75° half delta
	Error	Error	Error
α	$\pm 0.05^\circ$	$\pm 0.05^\circ$	$\pm 0.05^\circ$
δ	$\pm 0.2^\circ$	$\pm 0.2^\circ$	$\pm 0.2^\circ$
C_L	± 0.0015	± 0.0015	± 0.0015
C_L	± 0.010	± 0.010	± 0.010
C_h	± 0.010	± 0.011	± 0.006
C_{BM_F}	± 0.020	± 0.022	± 0.018

Because of the inaccuracies in the measurements by the optical system, the present control hinge-moment and bending-moment data do not warrant exact quantitative evaluation of the results. These inaccuracies are attributed to errors in manual control calibrations, dissimilar distortion of controls under actual aerodynamic loads and under calibrated loads, and errors arising from certain relations in the optics of the measuring system. A discussion of the latter error is given in reference 1. However on the basis of the repeated data, it appears that the estimates of the probable errors in C_{BM_F} and C_h given in the preceding table are reasonable.

RESULTS AND DISCUSSION

Figure 3 presents the basic aerodynamic coefficients at a Mach number of 1.96 plotted against angle of attack for the wing-fuselage combination with the control having 15° trailing-edge sweepback $\left(\frac{x_h}{\bar{c}_f} = 0.413\right)$.

~~CONFIDENTIAL~~

This control will hereafter be referred to as a 60° triangular control. These data are representative of the data for the other Mach numbers and tip controls which have been presented only in the form of cross plots in figures 4 to 15.

It will be noted in figure 3 that data were obtained for positive control deflections at both negative and positive angles of attack. Such data were used to obtain data for negative control deflections at positive angles of attack by reversing the signs of the angles and coefficients. This method of handling the data was possible because the model had symmetrical airfoil sections.

Effects of Plan Form With Fence Off

Hinge moments. - The variations of the hinge-moment coefficients with control deflections for the basic 60° half-delta control of reference 1, the 60° triangular control, and the 75° half-delta control are presented in figure 4 for angles of attack of 0° to 12°. At zero angle of attack the variation of hinge-moment coefficients with deflection tended to be fairly linear for the three control plan forms. Hinge-moment coefficients due to deflection at zero angle of attack were slightly underbalanced for the 60° and 75° half-delta controls with $\frac{X_h}{\bar{c}_f} = 0.455$, but the amount of underbalance for the 60° triangular control with $\frac{X_h}{\bar{c}_f} = 0.413$ was considerably greater.

As the angles of attack were increased, the variation of hinge-moment coefficients with control deflection became increasingly nonlinear for all three controls. The nonlinearities were such that the values of $C_{h\delta}$ which were zero or negative at positive deflections became positive for the 60° and the 75° half-delta controls as the control deflection decreased through zero. Values of $C_{h\delta}$ for the less closely balanced 60° triangular control generally increased positively as the control deflection decreased through zero but became positive only at 8° angle of attack for $M = 1.41$ and 12° angle of attack for $M = 1.62$. Data from tests of a similar wing-control configuration at $M = 1.61$ (ref. 4) showed similar hinge-moment nonlinearities existed when the control trailing edge was swept forward from 0° to -37.5°.

It is thus shown that the positive increases in $C_{h\delta}$ which occurred for the basic 60° half-delta control at moderate angles of attack as the control deflection was decreased near zero were not eliminated by increasing the control leading-edge sweep to 75°, by increasing the

control trailing-edge sweep to 15° , or by decreasing the control trailing-edge sweep to -37.5° . Reference 1 showed that these nonlinearities were apparently typical of controls having tip balance areas extending from the hinge line to the wing leading edge. Consequently, it appears that these nonlinearities are associated with the angular gap between the wing and control as the control unports.

Static hinge-moment and effectiveness data are not presented for the 45° half-delta control because of large torsional control vibration which occurred at angles of attack when the angle of attack was approximately equal to the control deflection but of opposite sign. Figure 5 was prepared to illustrate the angles of attack and deflections for which the vibrations occurred. In order to give some indication of the magnitude of the vibrations, three degrees of intensity were used, the rough index being the plus and minus change in indicated hinge moment from a neutral value. As the Mach number increased, the vibrations became less severe and within the range of conditions for which the vibration occurred, the intensity of the vibrations increased as the angle of attack decreased and as the deflection increased.

Values of the slope parameters C_{h_α} and C_{h_δ} for the 45° half-delta control, being unaffected by vibration at small angles of attack or small deflections, are presented in table I together with those for the 60° and 75° half-delta control. At all Mach numbers only small differences in C_{h_α} and C_{h_δ} were evidenced for these controls, which had

identical hinge-line locations $\left(\frac{x_h}{c_f} \approx 0.455\right)$, although the control

leading-edge sweep angle varied from 45° to 75° . Reasonable agreement with the experimental correlation of reference 4 (based on the ratio of balance area to total area for several tip controls) was also shown at $M = 1.62$ (see table I).

Control bending moments.— Bending-moment coefficients for the 60° triangular, and the 60° and 75° half-delta controls are presented in figure 6 cross plotted against deflection. In general, systematic variations of C_{BM_f} with angle of attack and deflection were noted for the three controls. For the 60° and 75° half-delta controls, the C_{BM_f} curves were more linear than those for the 60° triangular control. The magnitudes of C_{BM_f} for the 60° triangular and the 60° half-delta controls were about equal, and the magnitudes for the 75° half-delta control were about one third smaller than for the other two controls.

Rolling moment.— For zero angle of attack, rolling-moment coefficients increased with increasing deflection for the three plan forms (fig. 7). The rate of increase with deflection C_{l_δ} did not vary

appreciably with δ for the 60° triangular and 60° half-delta controls for zero angle of attack, but decreased considerably with increasing deflection for the 75° half-delta control at $M = 1.41$. Increasing the angle of attack or increasing the deflection at angles of attack above zero tended to decrease the parameter $C_{l\delta}$ for positive deflection.

For the 60° triangular and the 75° half-delta controls at $M = 1.41$, the decrease in $C_{l\delta}$ became progressively more pronounced until a value of deflection was reached (at $\alpha = 12^\circ$) beyond which further increases in deflection caused decreases in rolling moment. For the 60° half-delta control, similar results were shown in reference 1 for higher angles of attack. In the negative deflection range the changes in $C_{l\delta}$ with angle of attack were considerably less pronounced than at positive deflections, and were somewhat erratic. In general, the roll effectiveness $C_{l\delta}$ of the 60° half-delta control and the 60° triangular control were approximately equal, although the area of the 60° half-delta control was slightly smaller. The roll effectiveness for the 75° control was considerably less than for the other two controls, which was to be expected because of its smaller area. Rolling moment per unit area was, however, more nearly equal for all three controls at zero angle of attack - the 60° half-delta control having the highest effectiveness and the 75° half-delta the lowest. As the angle of attack was increased though, the loss in effectiveness per unit area for the 75° half-delta control was considerably greater than for the other two controls.

Incremental lift effectiveness. - The trends of the ΔC_L variations with angle of attack and deflection (fig. 8) were similar to those shown by the rolling-moment data. That is, $\Delta C_{L\delta}$ at positive deflections decreases with increases in angle of attack and deflection, and effects at negative deflections were much less pronounced.

Also values of ΔC_L were much less for the 75° half-delta control than for the other two controls, and were in general, about equal for the 60° half-delta and the 60° triangular controls.

Effects of Plan Form With Fence On

Data obtained with a fence installed at the wing control parting line are presented in figures 9 to 12 together with the fence-off data. It should be noted that the 60° triangular control used for the fence-on tests was slightly smaller and had a more rearward hinge-line location (see fig. 1) than the 60° triangular control used for fence-off tests. For this reason, the fence-on and fence-off data for these controls can be compared directly only insofar as trends are concerned.

In general, the data showed that addition of the fences caused no major change in the effects of plan form.

The hinge-moment data of figure 9 support the conclusions of references 1, 8, and 9 in that addition of the fence at the control parting line reduced the nonlinear variations of hinge moment with both angle of attack and deflection. It appears likely that the nonlinearities in the hinge-moment variation with deflection which occur at moderate to large angles of attack near zero deflection would have been reduced by use of a partial-chord fence extending only from the wing leading edge to the control hinge line. Data of references 8 and 9 show that similar nonlinear hinge-moment variations with deflection were successfully eliminated or delayed to higher angles of attack and more negative deflections by use of the partial chord fence on a horn-balanced flap-type control and a 60° half-delta control. These data indicate that these nonlinearities are associated principally with the gap between wing and tip balance area forward of the hinge line rather than with the plan form of the control.

The addition of the fence had only minor effects on the variation with deflection of C_{BM} , C_L and ΔC_L as shown by figures 10, 11, and 12, respectively.

Effects of Skewing Wing

Hinge moments.- Data of figure 13 show that, at low angles of attack, the shape of the curves for C_h against δ was changed considerably by $\pm 10^\circ$ wing skew, but that the magnitudes were not affected to any great extent. At higher angles of attack, however, skewing the wing forward at $M = 1.41$ caused increases in C_h at negative deflections, and skewing the wing backward at $M = 1.96$ caused large negative increases in C_h at positive deflections. Since the nonlinear characteristics of tip controls are not improved by changing either control leading-edge or trailing-edge sweep or by skewing the wing-control combination, it may be reasoned that no improvement would result if wing plan form were left unskewed while hinge line and parting line were skewed.

Bending moments.- In general, the data of figure 14 show that the slope of the curves for C_{BM_F} against deflection increases as the wing is skewed forward and decrease as the wing is skewed back. The data also show that the magnitudes of C_{BM_F} due to angle of attack at zero deflection increase as the wing is skewed forward and decrease as the wing is skewed back. The result is that maximum bending-moment coefficients are obtained at positive angles of attack and deflections for the wing in a skewed forward attitude.

Rolling moment. - The rolling-moment characteristics for zero angle of attack (fig. 15) indicate small increases in effectiveness with the wing skewed forward. At the higher angles of attack, the effect of skewing the wing forward was to cause a greater increase in effectiveness at negative deflections and a decrease in effectiveness at positive deflections. Skewing the wing back caused small decreases in effectiveness for all angles of attack at $M = 1.96$.

In considering the over-all roll effectiveness for a complete wing configuration with equal up and down deflection of opposite ailerons, the data at $M = 1.96$ indicate that the total roll effectiveness would be little affected by $\pm 10^\circ$ skew for zero angle of attack. However, at higher angles of attack, the roll effectiveness would be decreased if the down aileron was on the leading wing panel and would be increased if the down aileron was on the trailing wing panel.

CONCLUDING REMARKS

An investigation of tip controls on a 60° delta wing conducted in the 9- by 12-inch supersonic blowdown tunnel at Mach numbers of 1.41, 1.62, and 1.96 and supplemented by data from previous investigations indicated the following results:

1. The nonlinear hinge-moment variations with deflections characterized by a positive increase in the slope parameter $C_{h\delta}$ at moderate angles of attack as the deflection is decreased through zero are not improved when:

- (a) the control leading edge is sweptback 75°
- (b) the control trailing edge is sweptback 15°
- (c) the control trailing edge is sweptforward 37.5°
- (d) the control parting line and hinge line is skewed either 10° backwards or 10° forward.

These nonlinear variations are apparently associated principally with the gap between the wing and control forward of the hinge line since sealing the gap by a fence generally eliminates the nonlinearities.

2. The control effectiveness per unit area was little affected by increasing the control trailing-edge sweep to 15° , but was considerably decreased at angles of attack above zero by increasing the leading-edge sweep from 60° to 75° .

3. Values of the slope parameters $C_{h\alpha}$ and $C_{h\delta}$ at zero angle of attack and zero control deflection for the half-delta tip controls having hinge-line locations at 45.5 percent mean aerodynamic chord of control were essentially unchanged by variations of control leading-edge sweep from 45° to 75° .

4. Large torsional vibration occurred for the 45° half-delta control when the control deflection was approximately equal to the angle of attack but of opposite sign.

5. The skewed wing tests of a 60° half-delta control indicated that the only major effect of $\pm 10^\circ$ wing skew were large negative increases in hinge-moment coefficients at positive control deflections and high angles of attack for the skewed back condition.

Langley Aeronautical Laboratory,
National Advisory Committee for Aeronautics,
Langley Field, Va., September 24, 1953.

REFERENCES

1. Guy, Lawrence D.: Control Hinge-Moment and Effectiveness Characteristics of a 60° Half-Delta Tip Control on a 60° Delta Wing at Mach Numbers of 1.41 and 1.96. NACA RM I52H13, 1952.
2. Martz, C. William, Church, James D., and Goslee, John W.: Rocket-Model Investigation To Determine the Force and Hinge-Moment Characteristics of a Half-Delta Tip Control on a 59° Sweptback Delta Wing Between Mach Numbers of 0.55 and 1.43. NACA RM I52H06, 1952.
3. Martz, C. William, and Church, James D.: Flight Investigation at Subsonic, Transonic, and Supersonic Velocities of the Hinge-Moment Characteristics, Lateral-Control Effectiveness, and Wing Damping in Roll of a 60° Sweptback Delta Wing With Half-Delta Tip Ailerons (Revised). NACA RM I51G18, 1951.
4. Czarnecki, K. R., and Lord, Douglas R.: Hinge-Moment Characteristics for Several Tip Controls on a 60° Sweptback Delta Wing at Mach Number 1.61. NACA RM I52K28, 1953.
5. Burgess, Warren C., Jr., and Seashore, Ferris L.: Criterion for Condensation-Free Flow in Supersonic Tunnels. NACA TN 2518, 1951.
6. May, Ellery B., Jr.: Investigation of the Effects of Leading-Edge Chord-Extensions on the Aerodynamic and Control Characteristics of Two Sweptback Wings at Mach Numbers of 1.41, 1.62, and 1.96. NACA RM I50L06a, 1951.
7. Conner, D. William: Aerodynamic Characteristics of Two All-Movable Wings Tested in the Presence of a Fuselage at a Mach Number of 1.9. NACA RM I8H04, 1948.
8. Czarnecki, K. R., and Lord, Douglas R.: Preliminary Investigation of the Effect of Fences and Balancing Tabs on the Hinge-Moment Characteristics of a Tip Control on a 60° Delta Wing at Mach Number 1.61. NACA RM I53D14, 1953.
9. Guy, Lawrence D.: Control Hinge-Moment and Effectiveness Characteristics of a Horn-Balanced, Flap-Type Control on a 55° Sweptback Triangular Wing of Aspect Ratio 3.5 at Mach Numbers of 1.41, 1.62, and 1.96. NACA RM I52L15, 1953.

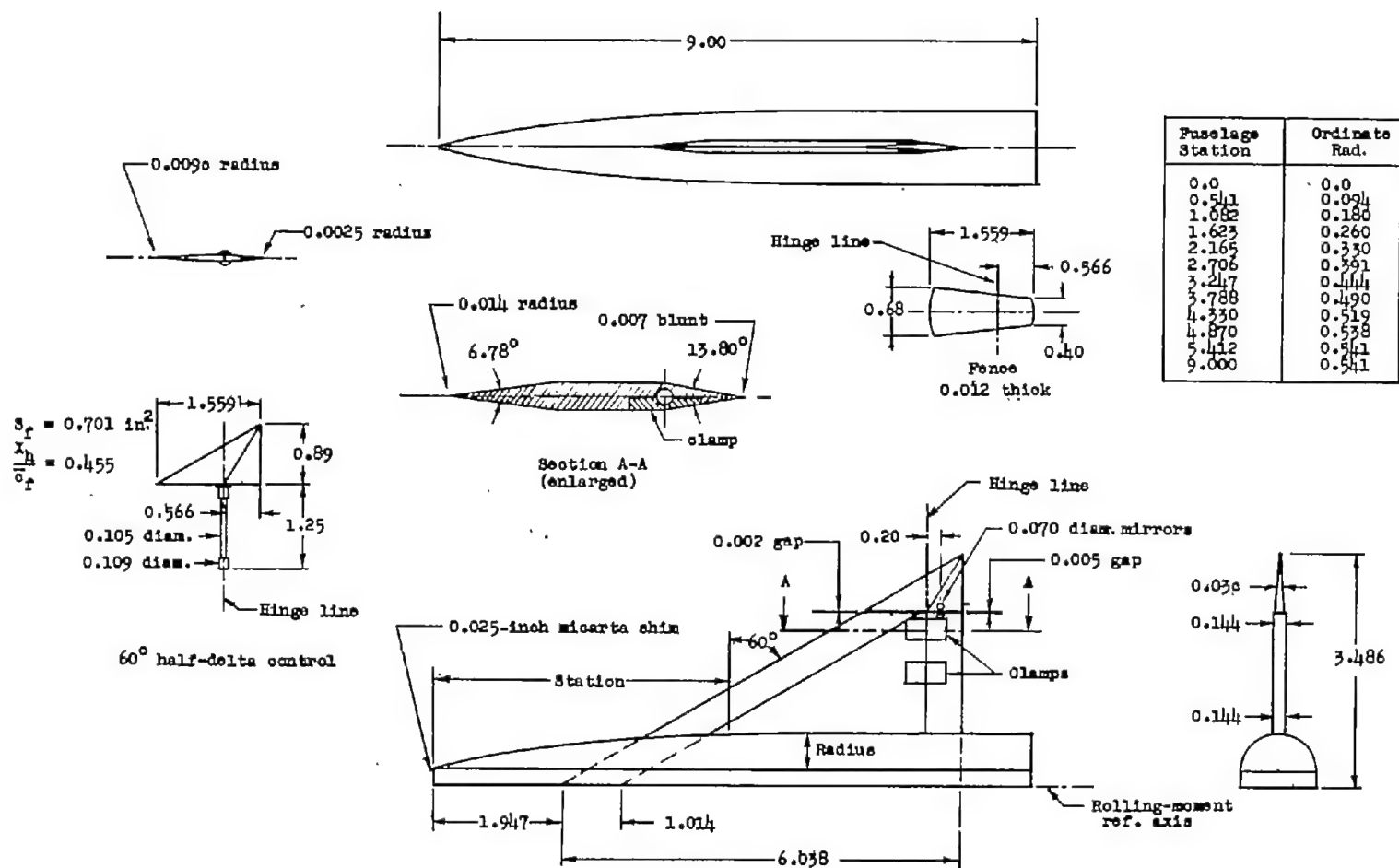
TABLE I

VALUES OF THE SLOPE PARAMETERS $C_{h\alpha}$ AND $C_{h\delta}$ AT ZERO ANGLE

OF ATTACK AND DEFLECTION FOR HALF-DELTA TIP CONTROLS

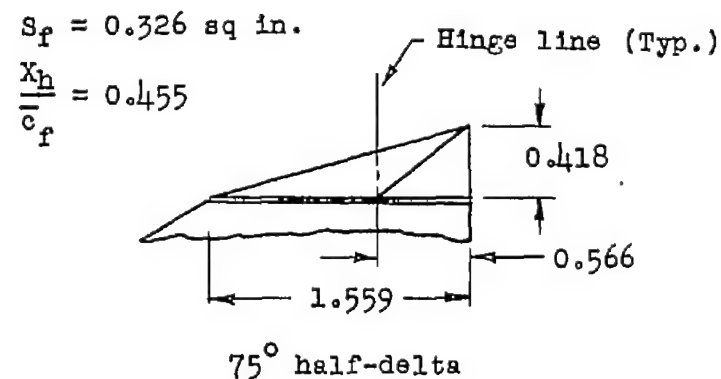
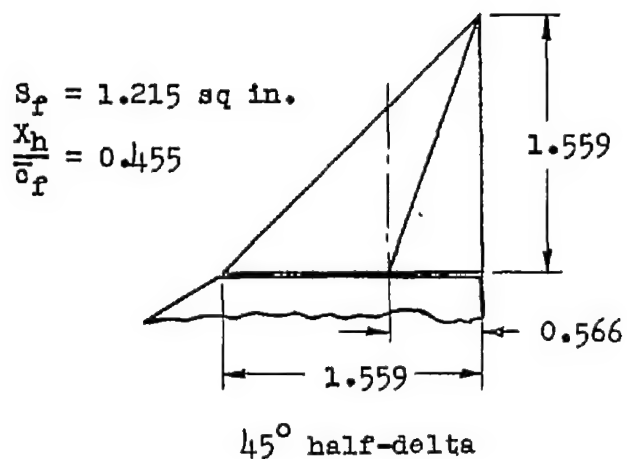
HAVING HINGE-LINE LOCATIONS AT $\frac{x_h}{\bar{c}_f} = 0.455$

Control leading- edge sweep, (deg)	M = 1.41		M = 1.62		M = 1.96	
	$C_{h\alpha}$	$C_{h\delta}$	$C_{h\alpha}$	$C_{h\delta}$	$C_{h\alpha}$	$C_{h\delta}$
45	0.0015	-0.0015	0.00170	0	0.00170	-----
60	.00250	-.0011	.00310	-0.0010	.00320	-0.0011
75	.00120	-.0005	.00125	0	.00450	-.00075
Experimental correlation of reference 4	-----	-----	.0030	.0008	-----	-----

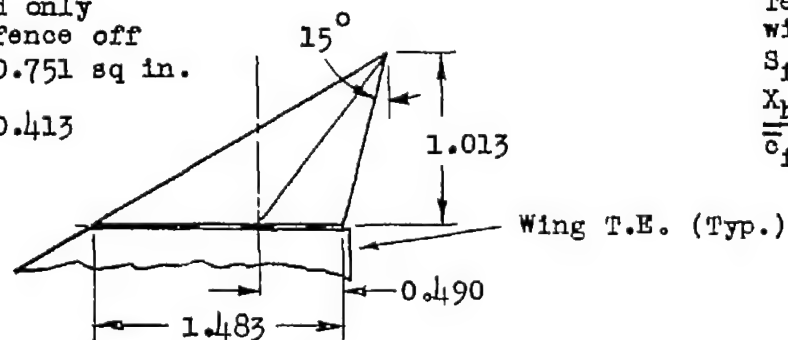


(a) Basic model showing 60° half-delta control.

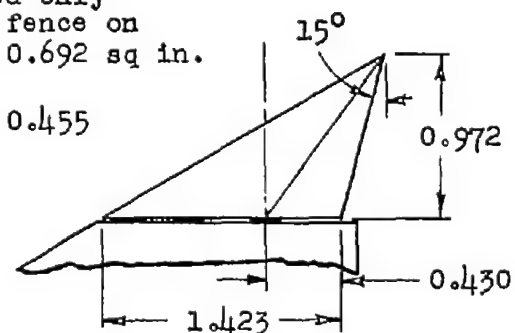
Figure 1.- Details of semispan-wing-fuselage combination. Aspect ratio, 2.3; mean aerodynamic chord, 4.025 inches; half wing area, 10.524 square inches. All dimensions are in inches.



Tested only
 with fence off
 $S_f = 0.751 \text{ sq in.}$
 $\frac{X_h}{c_f} = 0.413$



Tested only
 with fence on
 $S_f = 0.692 \text{ sq in.}$
 $\frac{X_h}{c_f} = 0.455$

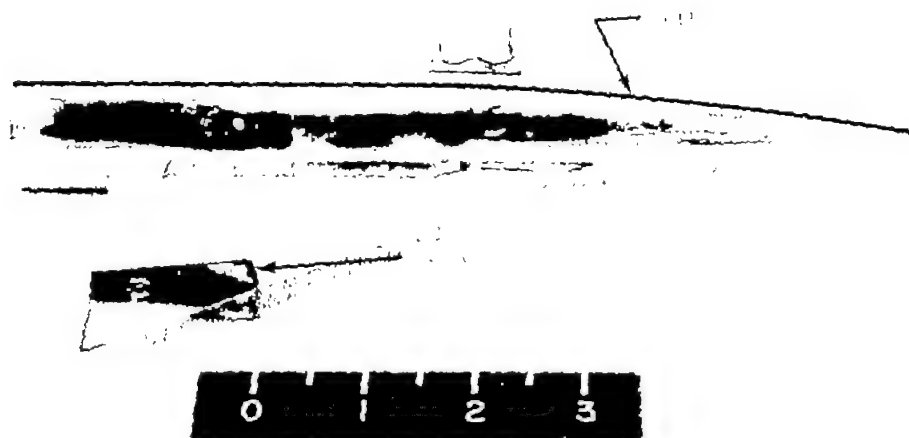


(b) Details of tip controls. All dimensions are in inches.

Figure 1.- Concluded.

3B

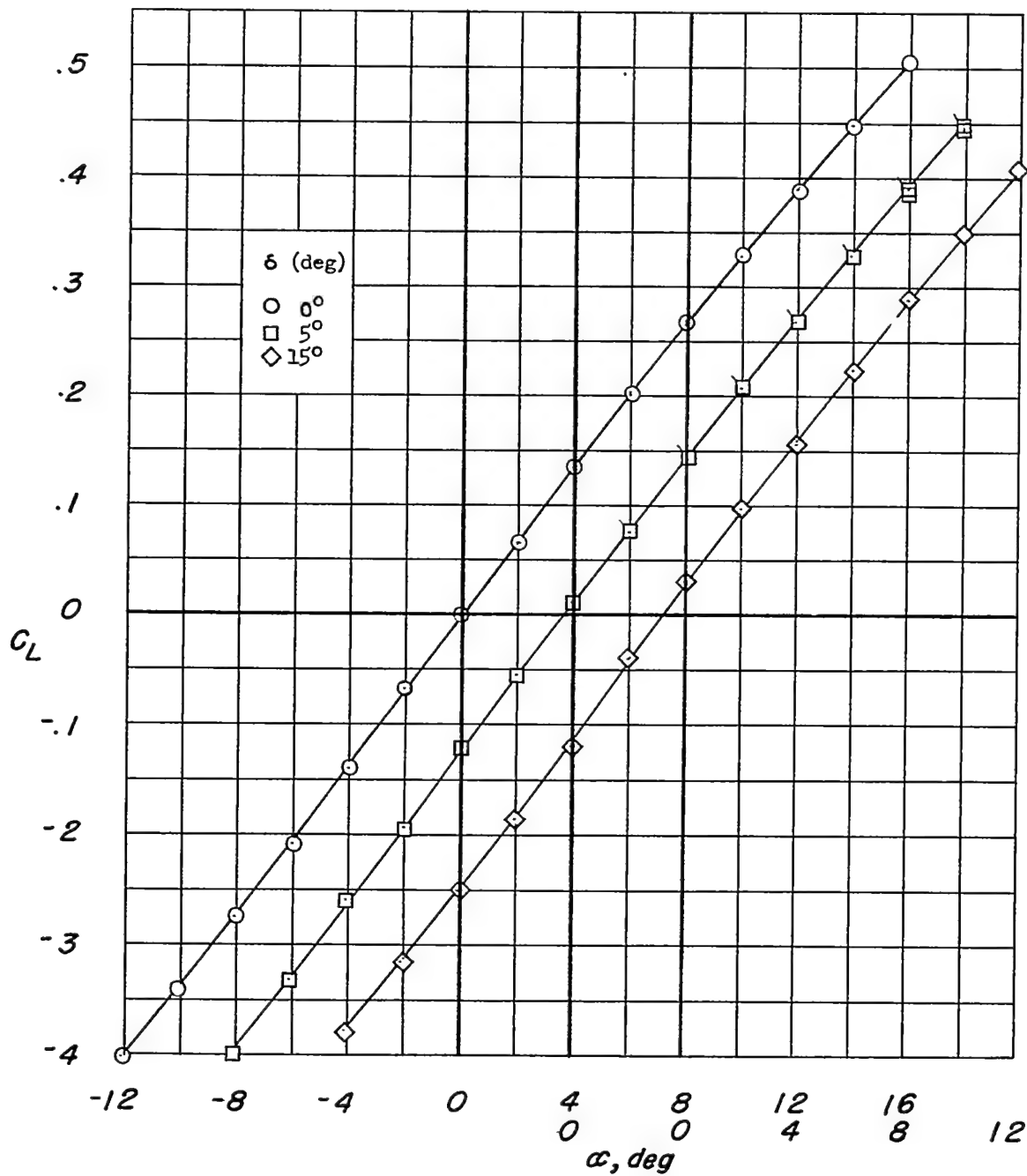
NACA RM 153708a



L-74730.1

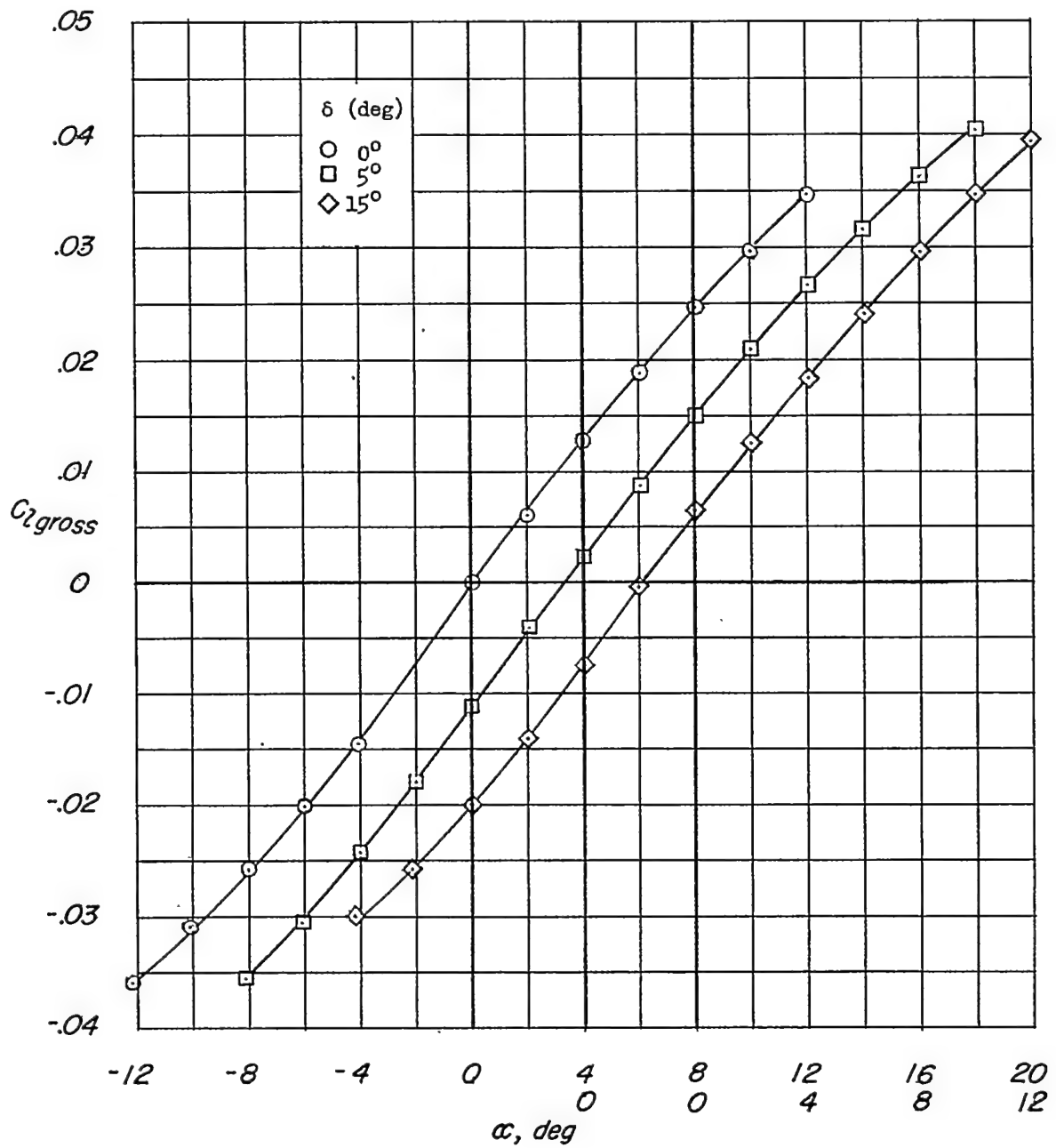
17

Figure 2.- Photograph of test model.



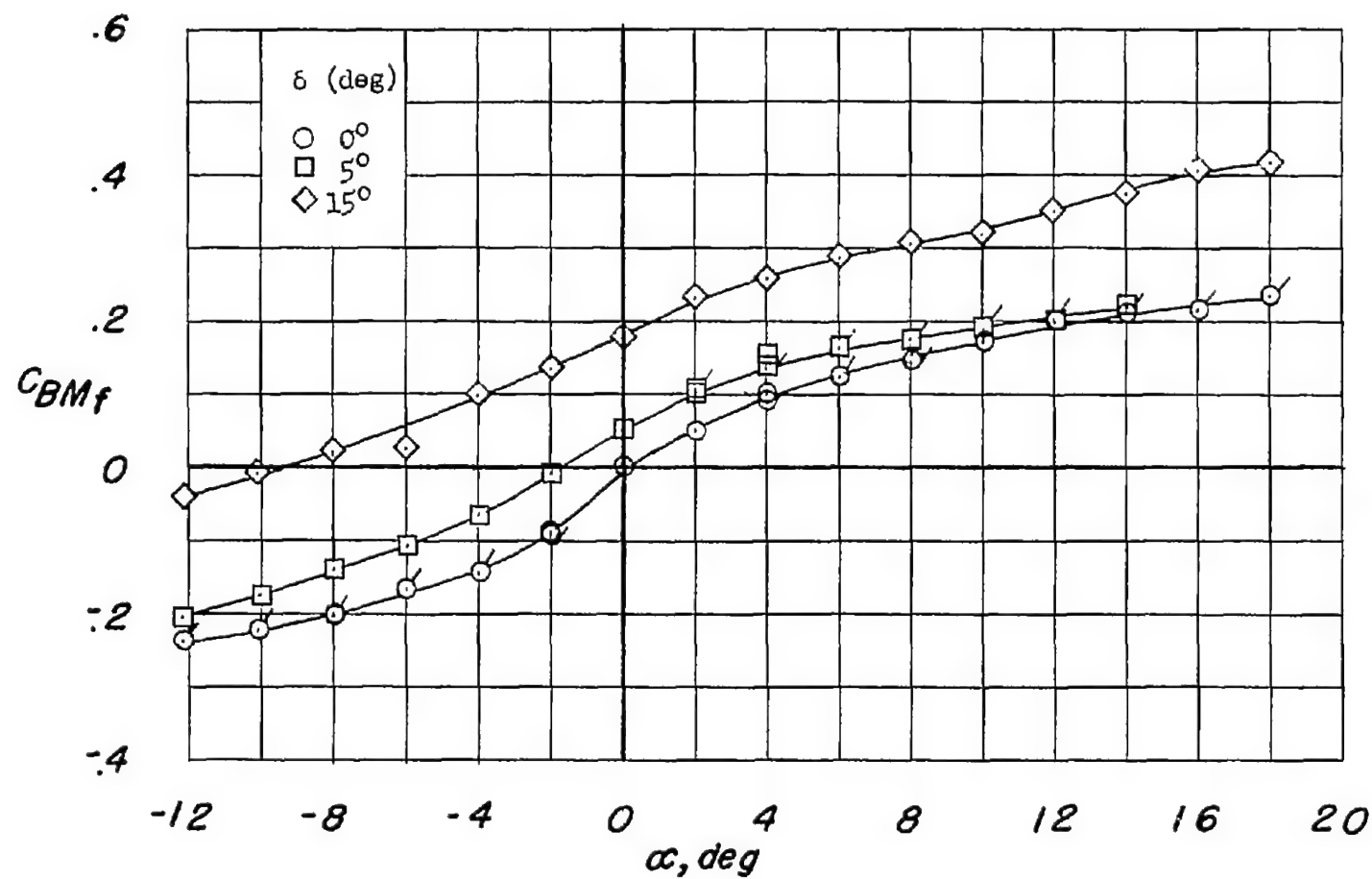
(a) C_L plotted against α .

Figure 3.- Aerodynamic characteristics of a 60° triangular control on a semispan delta-wing-fuselage combination. $\frac{x_h}{c_f} = 0.413$; $R = 2.0 \times 10^6$; $M = 1.96$; flagged symbols denote repeat tests.



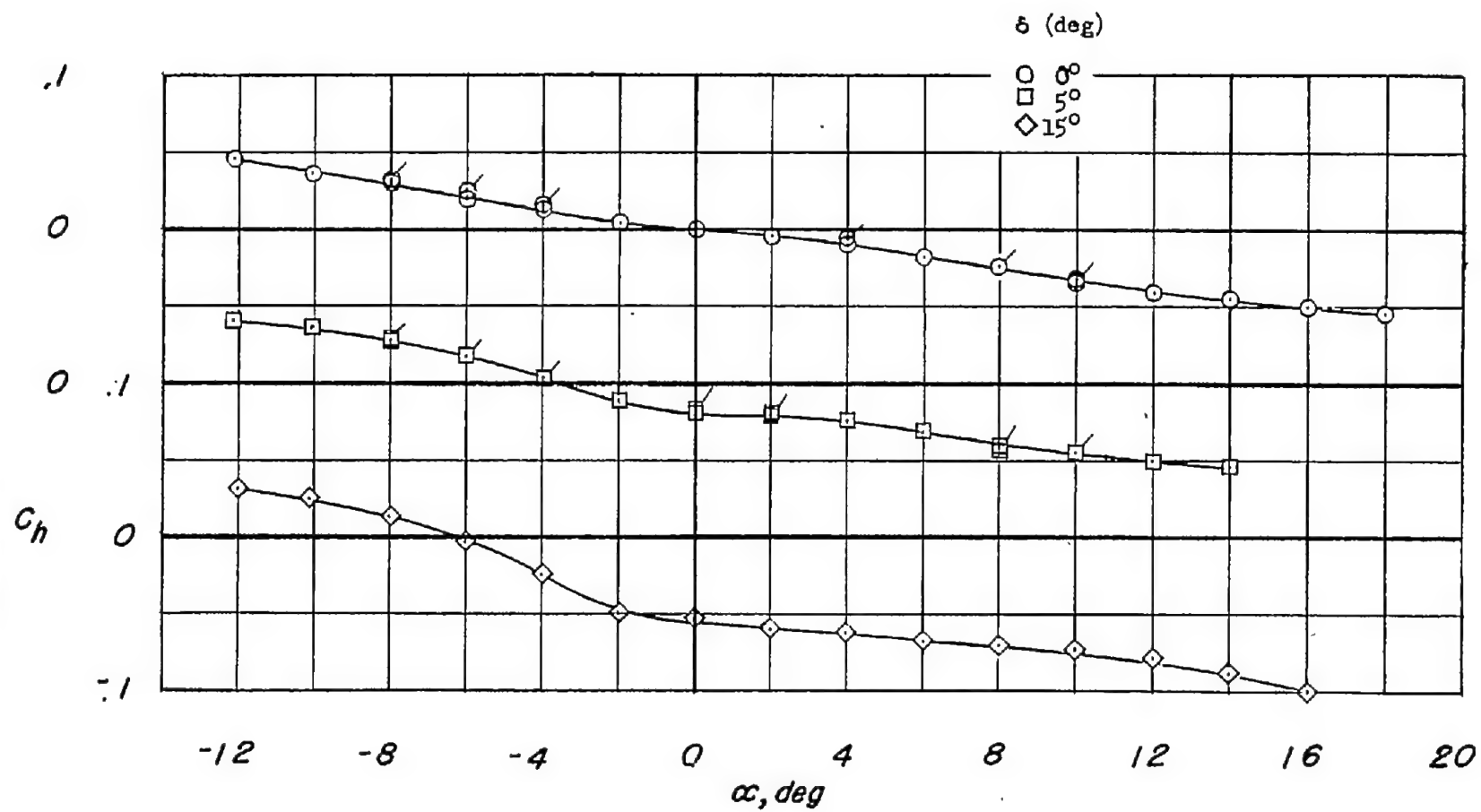
(b) $C_{L_{gross}}$ plotted against α .

Figure 3.- Continued.



(c) C_{BM_f} plotted against α .

Figure 3.- Continued.



(d) C_h plotted against α .

Figure 3.- Concluded.

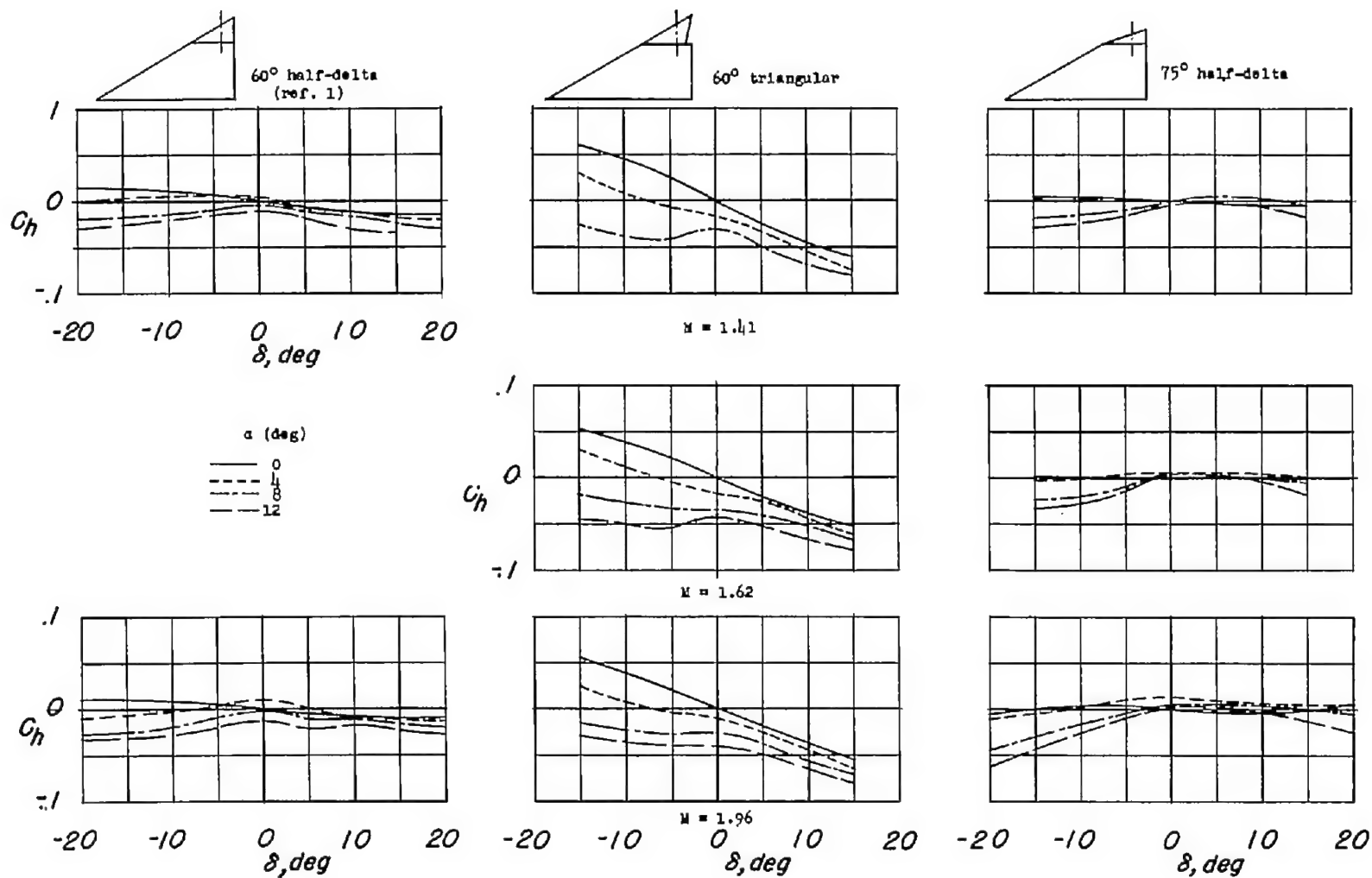
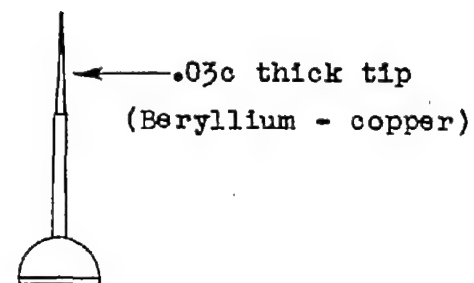
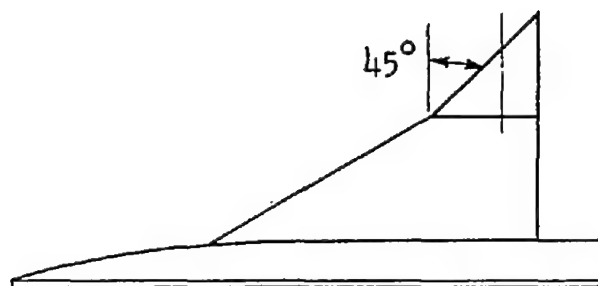
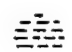




Figure 4.- Variation of hinge-moment coefficients with deflection for tip controls of three plan forms. $R = 2.4 \times 10^6$, 2.25×10^6 , and 2.0×10^6 ; $M = 1.41$, 1.62 , and 1.96 , respectively.



Vibration

-  Slight $\Delta C_h < \pm .02$
-  Moderate $\Delta C_h \approx \pm .06$
-  Severe $\Delta C_h > \pm .15$

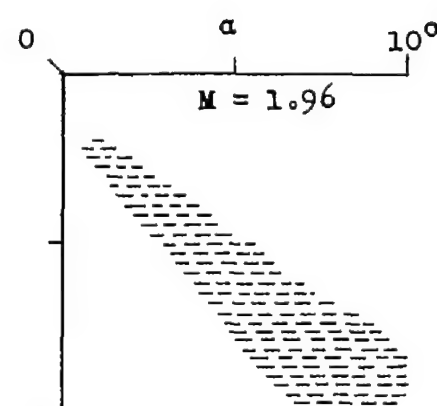
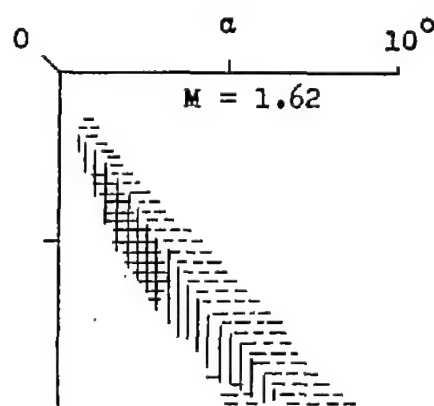
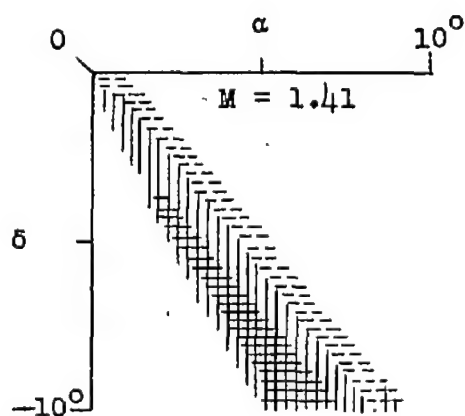


Figure 5.- Vibration of 45° half-delta tip control.

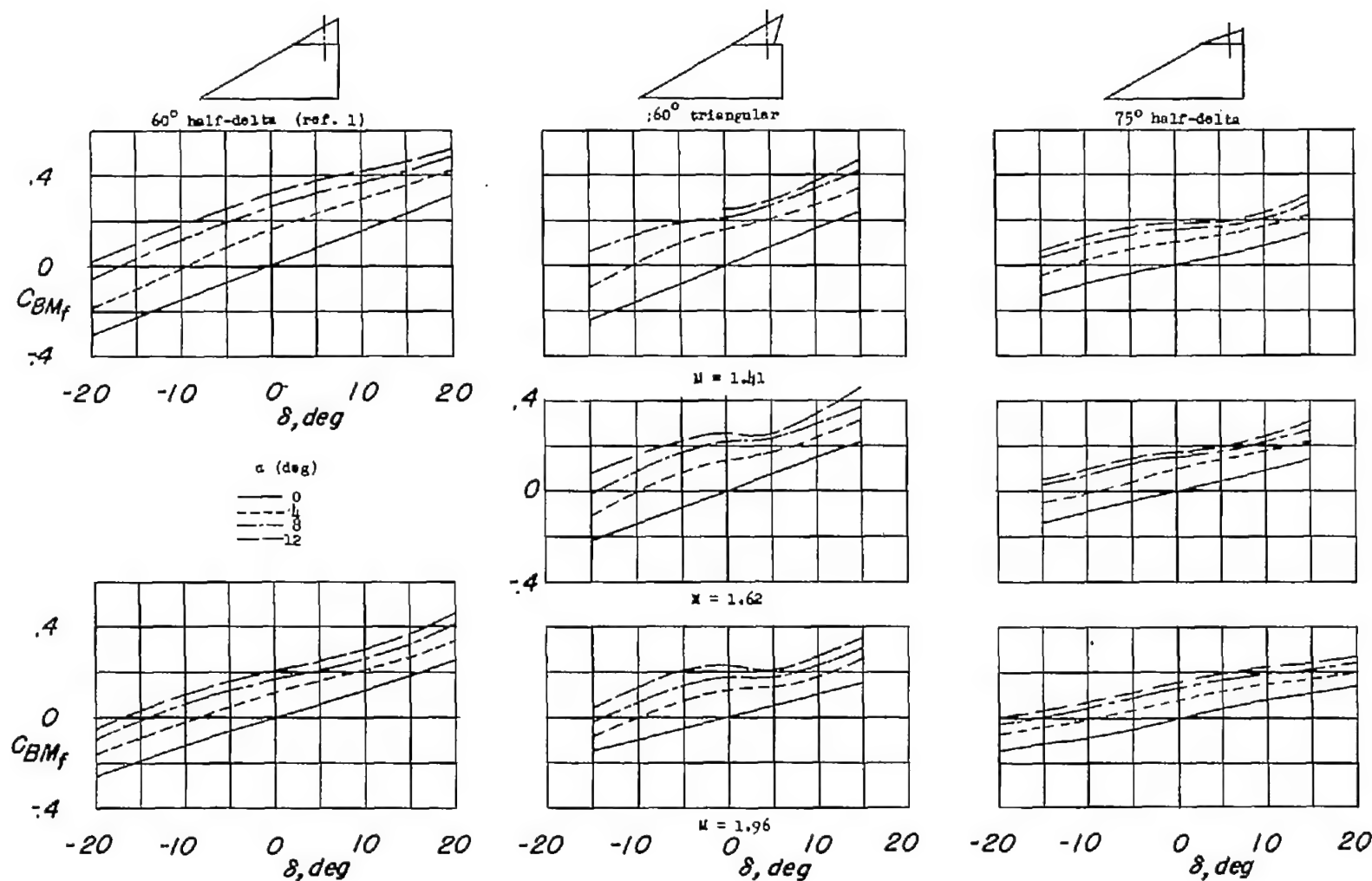


Figure 6.- Variation of bending-moment coefficient with deflection for tip controls of three plan forms. $R = 2.4 \times 10^6$, 2.25×10^6 , and 2.0×10^6 ; $M = 1.41$, 1.62 , and 1.96 , respectively.

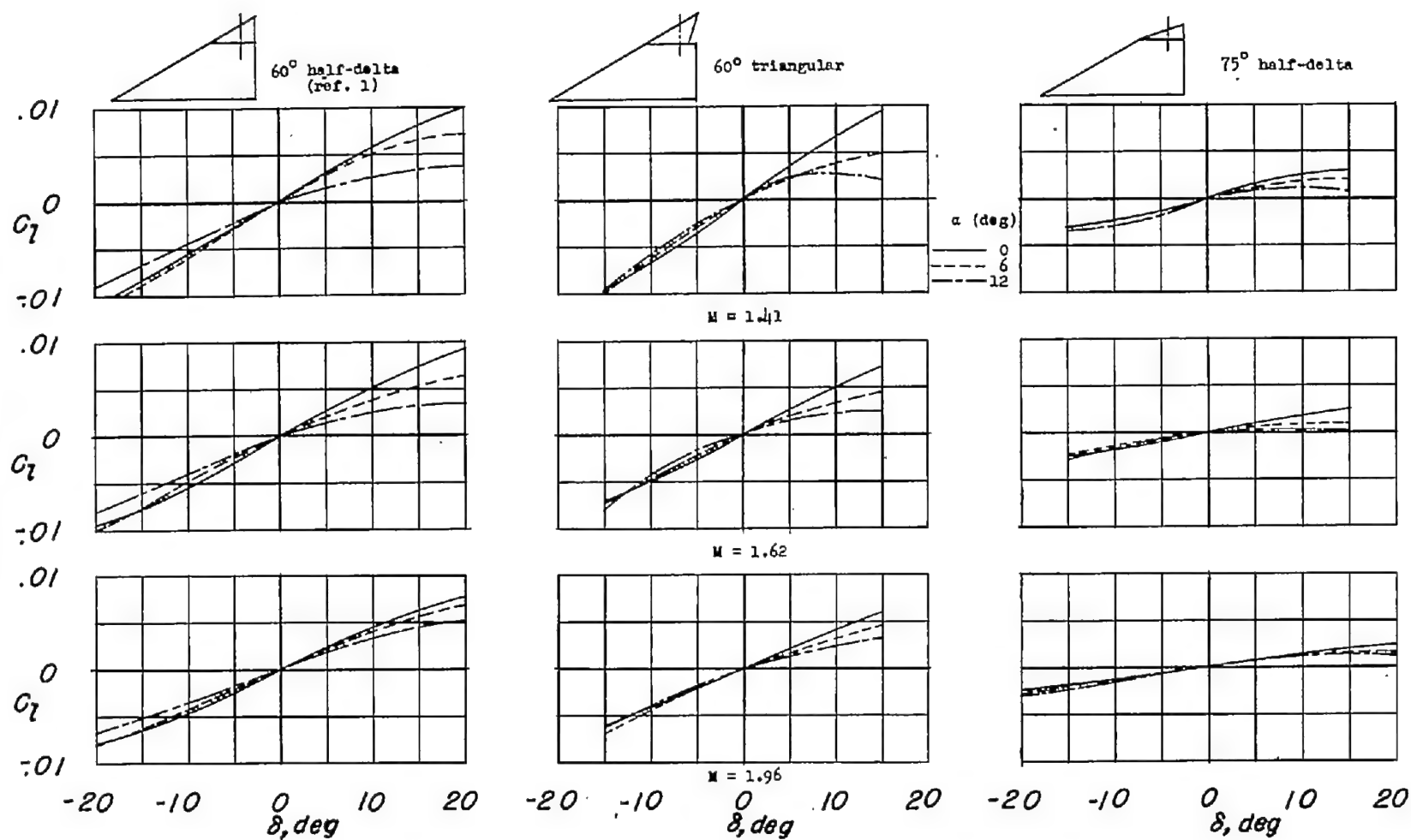


Figure 7.- Variation of rolling-moment coefficient with deflection for tip controls of three plan forms. $R = 2.4 \times 10^6$, 2.25×10^6 , and 2.0×10^6 ; $M = 1.41$, 1.62 , and 1.96 , respectively.

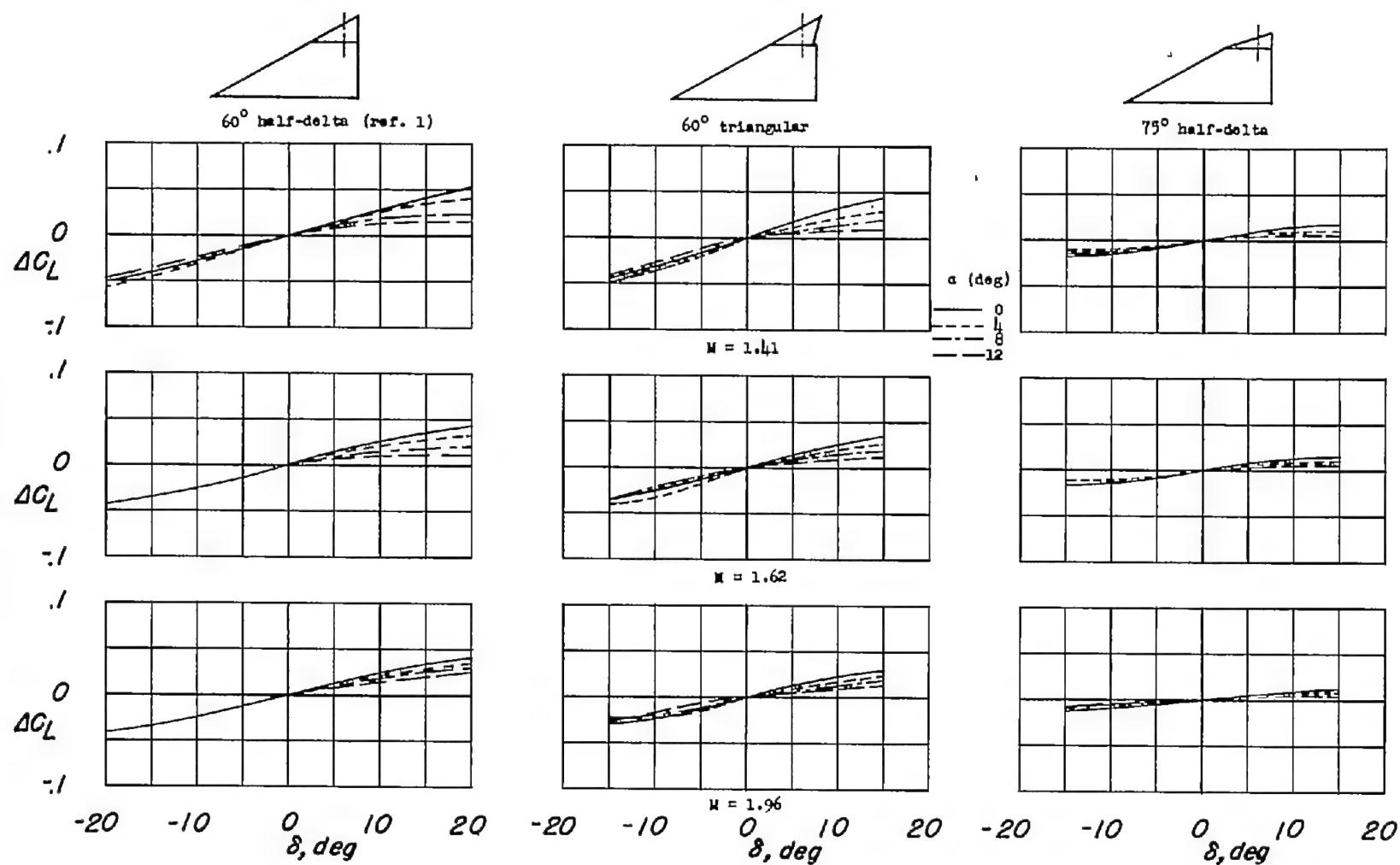


Figure 8.- Variation of the increments of lift coefficient with deflection for tip controls of three plan forms. $R = 2.4 \times 10^6$, 2.25×10^6 , and 2.0×10^6 ; $M = 1.41$, 1.62 , and 1.96 , respectively.

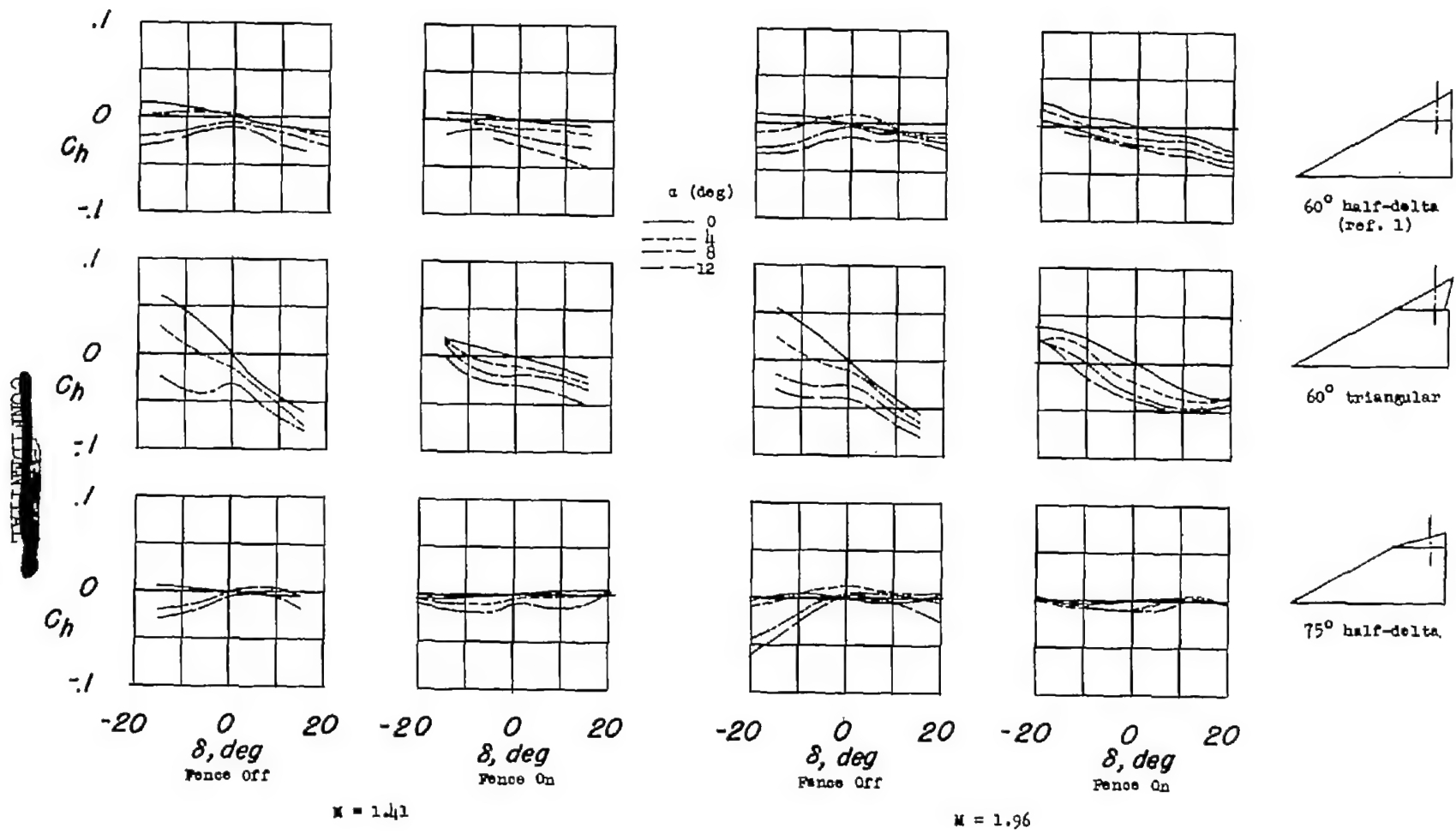


Figure 9.- Comparison of hinge-moment coefficients with and without fence for tip controls of three plan forms. $R = 2.4 \times 10^6$ and 2.0×10^6 ; $M = 1.41$ and 1.96 , respectively.

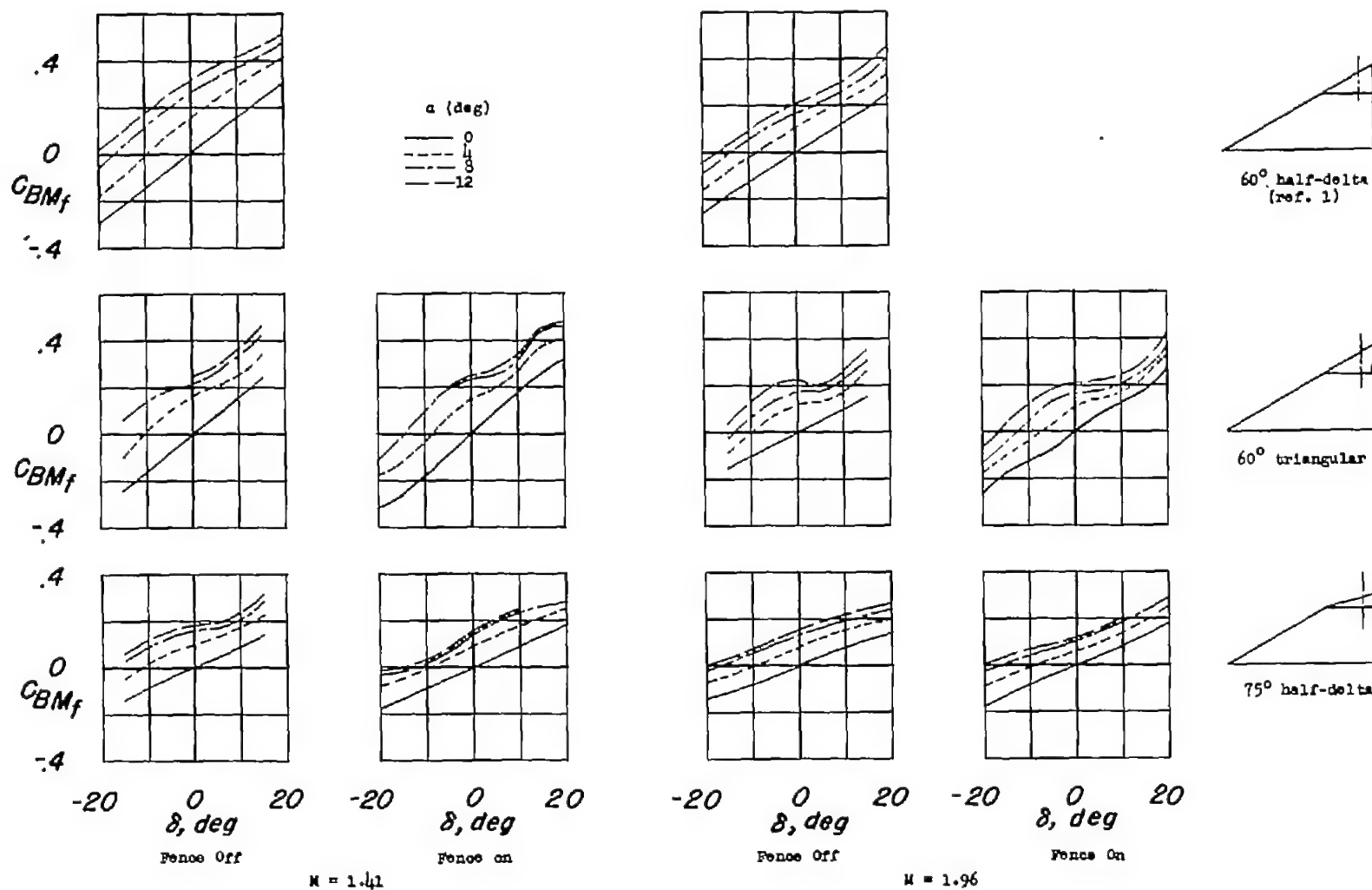


Figure 10.- Comparison of bending-moment coefficients with and without fence for tip controls of three plan forms. $R = 2.4 \times 10^6$ and 2.0×10^6 ; $M = 1.41$ and 1.96 , respectively.

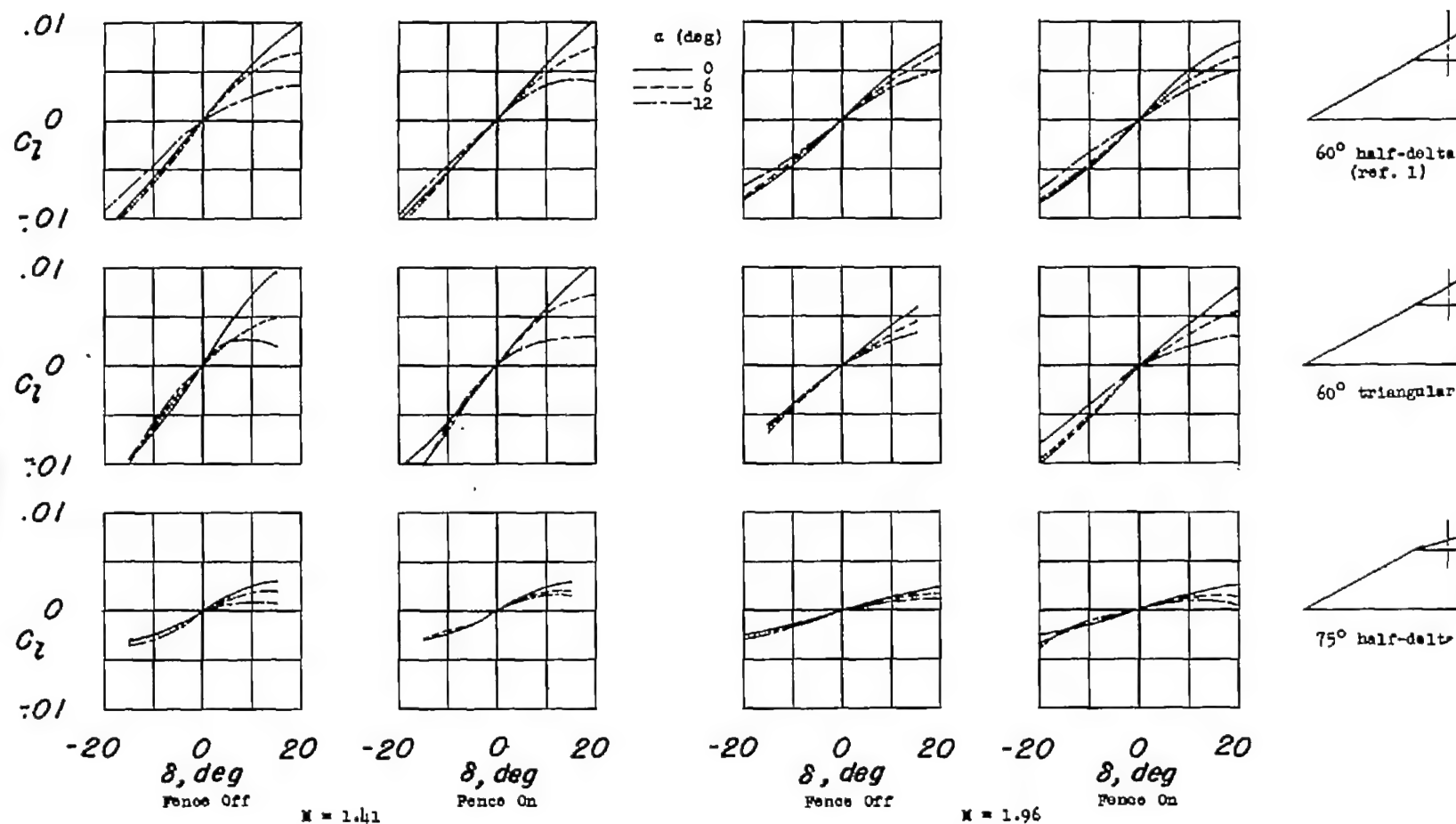


Figure 11.- Comparison of rolling-moment coefficients with and without fence for tip controls of three plan forms. $R = 2.4 \times 10^6$ and 2.0×10^6 ; $M = 1.41$ and 1.96 , respectively.

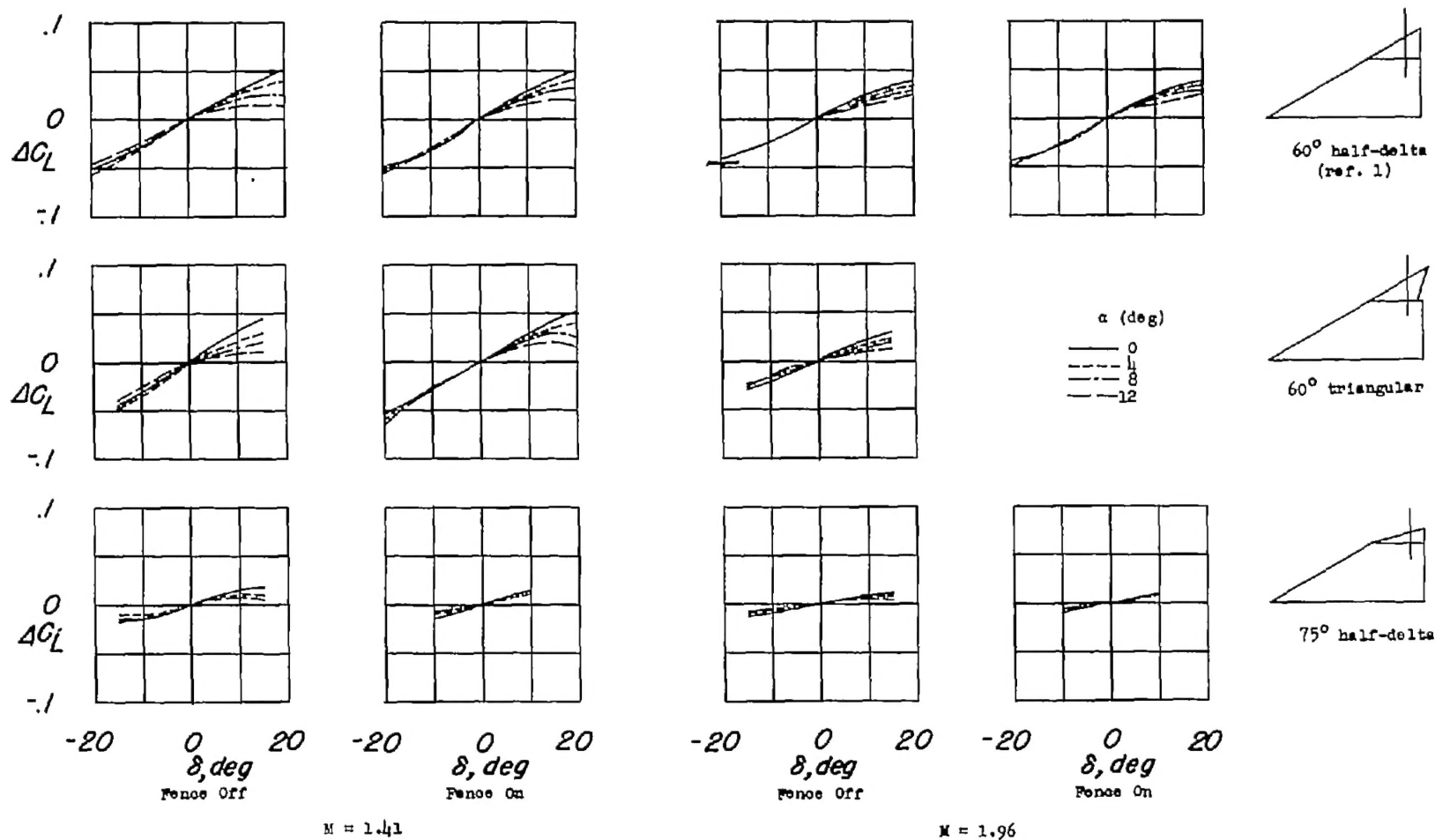


Figure 12.- Comparison of the increments of lift coefficients with and without fence for tip controls of three plan forms. $R = 2.4 \times 10^6$ and 2.0×10^6 ; $M = 1.41$ and 1.96 , respectively.

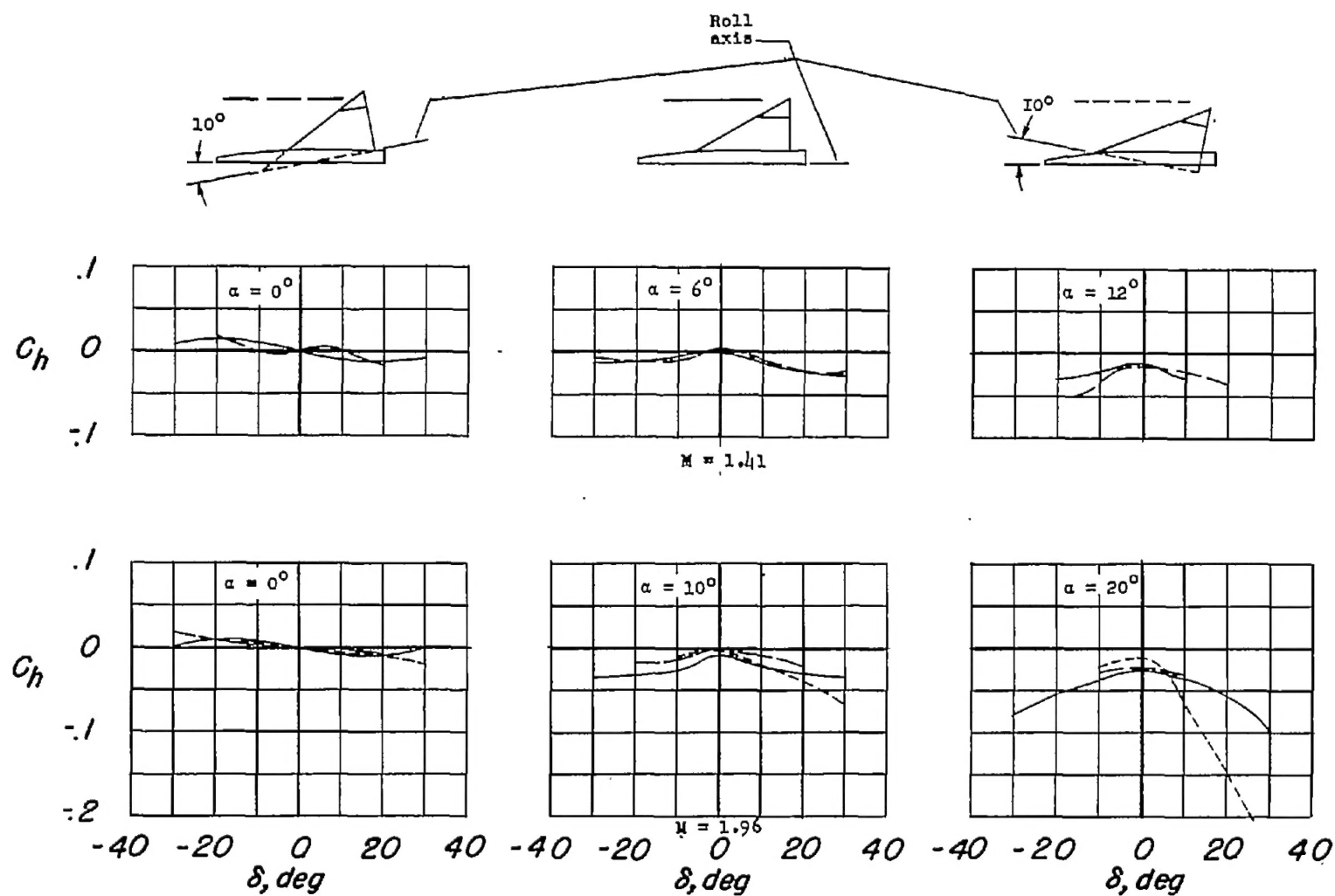


Figure 13.- Effects of wing skew on the variation of hinge-moment coefficient with deflection for a 60° half-delta control. $R = 2.4 \times 10^6$ and 2.0×10^6 ; $M = 1.41$ and 1.96 , respectively.

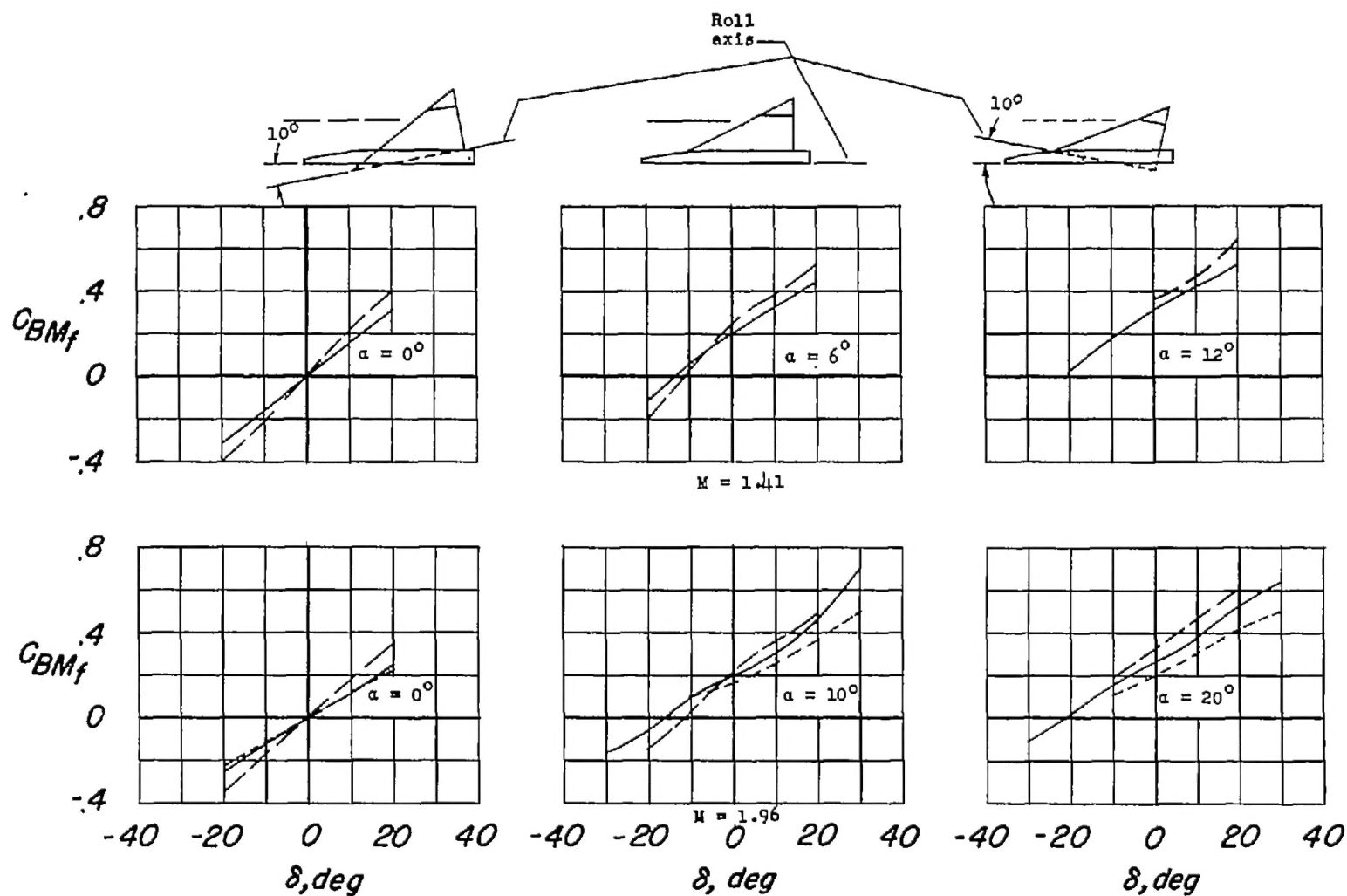


Figure 14.- Effects of wing skew on the variation of bending-moment coefficient with deflection for a 60° half-delta control. $R = 2.4 \times 10^6$ and 2.0×10^6 ; $M = 1.41$ and 1.96 , respectively.

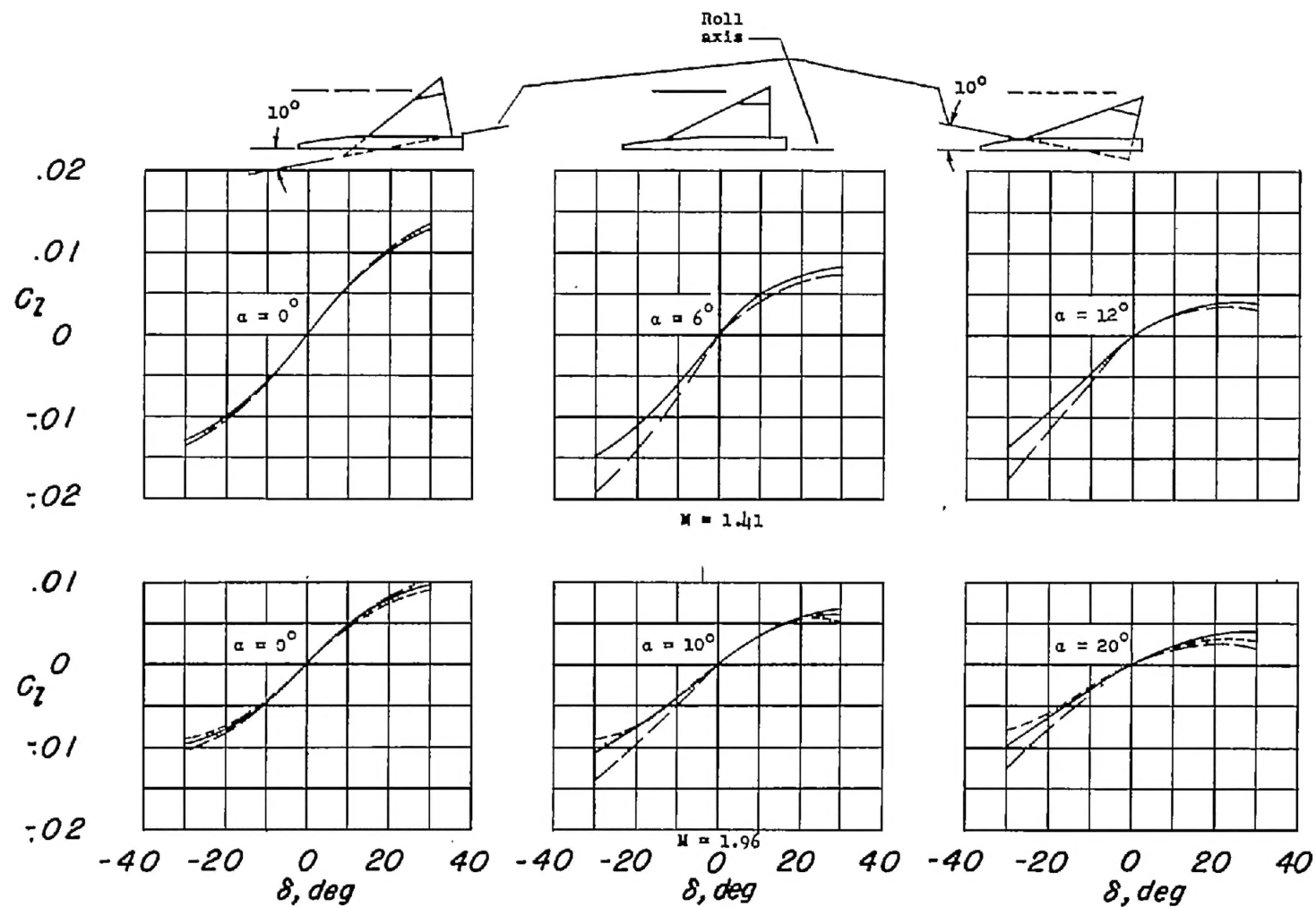


Figure 15.- Effects of wing skew on the variation of rolling-moment coefficient with deflection for a 60° half-delta control. $R = 2.4 \times 10^6$ and 2.0×10^6 ; $M = 1.41$ and 1.96 , respectively.